

Article

Comprehensive Analysis of Transient Overvoltage Phenomena for Metal-Oxide Varistor Surge Arrester in LCC-HVDC Transmission System with Special Protection Scheme

Jaesik Kang 

Korea Electrotechnology Research Institute, Gwangju 61751, Korea; jskang84@keri.re.kr; Tel.: +82-062-606-7277

Abstract: This paper proposes a systematic and deterministic method for metal-oxide varistor (MOV) surge arrester selection based on the comprehensive analysis in line-commutated converter (LCC)-based high-voltage direct current (HVDC) transmission systems. For the MOV surge arrester, this paper investigates several significant impacts on the transient overvoltage (TOV) phenomena, which is affected by practical factors such as an operating point of the LCC-HVDC system, synchronous machine operating status of the power system, AC passive filter trip, and communication delay in a special protection system (SPS). In order to determine an appropriate rating of surge arrester, especially for TOV, this paper considers a pattern, magnitude, and duration of TOV based on various fault scenarios in an electrical power system with an LCC-HVDC system. A screening study method with 60 Hz and RMS-based balance system is conducted for examining a wide range of fault scenarios, and then for the specific test cases that need a detailed analysis, electro-magnetic transient (EMT)-based analysis models are developed with an approvable boundary setting method through the equivalent network translation tool. A detailed EMT study is subsequent based on the distinguished cases; as a result, the exact number of metal-oxide resistor stacks could be obtained through the detailed TOV study according to this procedure. The efficacy of the selection method from the proposed procedure based on the comprehensive analysis are verified on a specific power system with a 1.5 GW DC \pm 500 kV symmetric monopole LCC-HVDC transmission system.

Keywords: metal-oxide varistor (MOV) surge arrester; temporary transient overvoltage (TOV); LCC-HVDC; special protection system (SPS); PSCAD/EMTDC



Citation: Kang, J. Comprehensive Analysis of Transient Overvoltage Phenomena for Metal-Oxide Varistor Surge Arrester in LCC-HVDC Transmission System with Special Protection Scheme. *Energies* **2022**, *15*, 7034. <https://doi.org/10.3390/en15197034>

Academic Editors: Xinran Zhang, Lipeng Zhu and Yue Song

Received: 5 August 2022

Accepted: 21 September 2022

Published: 25 September 2022

Publisher's Note: MDPI stays neutral with regard to jurisdictional claims in published maps and institutional affiliations.



Copyright: © 2022 by the author. Licensee MDPI, Basel, Switzerland. This article is an open access article distributed under the terms and conditions of the Creative Commons Attribution (CC BY) license (<https://creativecommons.org/licenses/by/4.0/>).

1. Introduction

Conventional power systems are rapidly changing, so that AC electrical networks experience fault current variations and stability degradation due to the high penetration of renewable energy sources (RESs) and high load density on specific regions such as metropolitan areas [1–6]. To resolve these problems, we could address them through potential solutions such as AC infrastructure expansion and T&D supportive equipment installation, which should be necessary; however, this would be practically impossible owing to social acceptability (social disapproval) [7–13]. Meanwhile, the high-voltage direct current (HVDC) transmission system is a very attractive alternative for transmission system operator (TSO) both to enhance the power system stability even with a penetration level increase of RES and to mitigate overloading condition over a specific location without social issues [14–19]. The HVDC system is an enabling technology for the AC/DC grid that allows a hybrid network to be compatible with highly level RESs penetration into a traditional power system topology [20–25].

The HVDC system could be realized with line-commutated converter (LCC) and modular multilevel converter (MMC) as a voltage-sourced converter (VSC), respectively. The LCC-HVDC system is based on a thyristor switching device available for current commutation mode. The thyristor-based LCC-HVDC system causes a phase difference

between current and voltage due to unidirectional conduction and non-forced blocking capability, and hence it generates an inductive reactive power consumption [26,27]. On the other hand, the MMC-HVDC system is based on the VSC with an insulated gate bipolar transistor (IGBT) switching device, which is capable of bi-directional current conduction and independently controlling real and reactive power [28]. Nonetheless, the LCC-HVDC transmission system has been evolving as an enabling technology for transmitting bulk power in a large power system, because a large power delivery could be achieved through a high-capacity thyristor switching device [29]. However, LCC-HVDC system obviously needs an additional passive filter to compensate the harmonics and reactive power absorption as mentioned above [30].

In the South Korean power system, an LCC-HVDC transmission system would be expected to be installed on the mainland to supply the bulk power produced from offshore wind farms and large complex plants into a critical capital region and manufacturing facility via long-distance lines [31–33]. In particular, it is important to achieve the reliability, security, and resiliency of the LCC-HVDC system for the Korean electric power system under a lack of AC transmission line for large power-generation systems [34–37]. For such an inevitable power system condition, there were studies on a stable management and operation against resonance issues between generators and AC filters of the LCC-HVDC system [38–43], and also several power system analyses and research studies were conducted [44–48]. During the severe faults under the condition, however, the passive filter for reactive power compensation causes temporary transient overvoltage (TOV) variations due to its shortly persistent operating situation even after the generator and HVDC system trip. This important issue has not yet been investigated thoroughly.

An accurate metal-oxide varistor (MOV) surge arrester should be installed on the power system to protect the LCC-HVDC system from the generated transient overvoltage. There have been previous studies on the surge arrester for the protection and insulation coordination with respect to transient overvoltage [49–51]; however, the characteristics are steadily changing owing to an advent of FACTS and HVDC applications based on power electronic system into the conventional power grid. Hence, the specific research on analysis of surge arrester determination with discharge energy related to DC fault conditions on MMC-HVDC systems has been conducted [52], and the general research on the surge arrester and transient overvoltage in HVDC systems has been studied [53–56]. However, there have not yet been investigations or a detailed analysis for MOV surge arrester selection considering the major practical and physical concerns, such as AC power system configuration, generators, and HVDC operating conditions, passive filter state, trip and communication time delay, and so on. In other words, it should be required for comprehensive analysis to determine the MOV surge arrester with relation to various factors in power systems connected to the LCC-HVDC system.

This research analyzes transient overvoltage phenomena with various sensitive factors in the LCC-HVDC transmission system, and an accurate surge arrester selection procedure is proposed based on the comprehensive analysis. For the MOV surge arrester determination, a screening study and detailed EMT simulations are conducted; as a result, an enhanced protection and insulation coordination for LCC-HVDC system can be achieved through analysis of magnitude, pattern, and duration of TOV generated by critical fault cases. In this paper, Section 2 introduces a specific electric power system for applying with MOV surge arrester connected with point-to-point LCC-HVDC transmission system. Then, fundamental information regarding the MOV surge arrester is briefly described in Section 3. Subsequently, a screening study and an EMT-based detailed analysis are carried out to examine TOV and select the required surge arrester, and thus the analytic results verify that the determination method is demonstrated for the MOV surge arrester with respect to temporary transient overvoltage corresponding to the number of generators, communication delay, the number of passive filters, and HVDC operating point, etc. Finally, the conclusions of this paper are summarized in Section 4.

2. Power System and LCC-HVDC Configuration

Figure 1 illustrates the specific electric power system connected by LCC-HVDC transmission system. Three generators described in Table 1 are connected at bus 2. The #2CC and #4CC consist of gas and steam turbines in a 2:1 ratio, and the #3CC provides 422.75 MW to the grid. A static synchronous compensator (STATCOM) installed at bus 3 regulates the system-operating voltage through reactive power support. As seen in Figure 1, the LCC-HVDC transmission system is connected between bus 2 and bus 3 to deliver the active power from the large power plants to the right side of the grid. Due to social acceptability issues in the region, an AC transmission line expansion plan is delayed between bus 2 and bus 3, and hence the only LCC-HVDC system becomes a main connection path for transmitting the bulk power produced from three large power plants to the right side of grid. The LCC-HVDC system is 1.5 GW and a DC ± 500 -kV monopole symmetric topology. In addition, the AC filters are installed at buses 2 and 3, respectively, for compensating the harmonics and injecting capacitive reactive power, and the details of the passive filters corresponding to the LCC-HVDC operating points are described in Table 2.

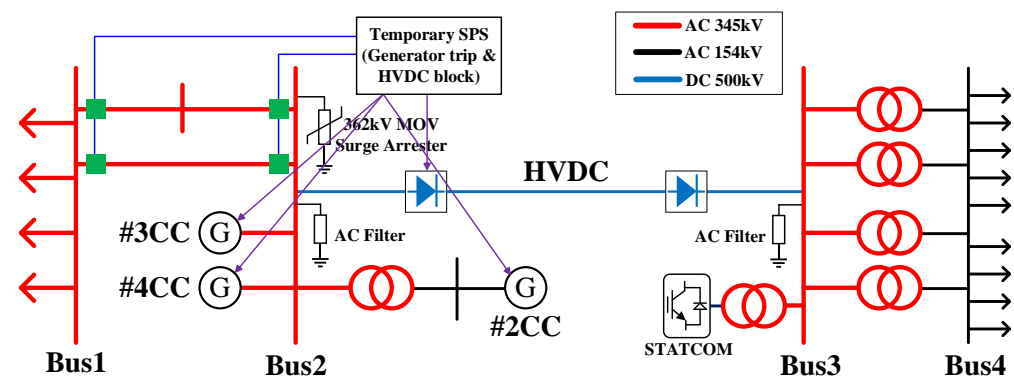


Figure 1. Schematic of the specific power system for analysis of temporary transient overvoltage (TOV) phenomena with respect to MOV surge arrester in line-commutated converter (LCC)-HVDC transmission system.

Table 1. Description of turbine generators.

Location	Generator	Capacity (MW)
#2CC at 154 kV	Gas Turbine (GT3)	185.25
	Gas Turbine (GT4)	185.25
	Steam Turbine (ST2)	187.15
#4CC at 345 kV	Gas Turbine (GT6)	295.45
	Gas Turbine (GT7)	295.45
	Steam Turbine (ST4)	296.40
#3CC at 345 kV	Gas & Steam Turbine	422.75

Table 2. Description of AC filter injection corresponding to LCC-HVDC system.

Operating Point	Capacity	The Number of AC Filter Injection at Bus 2 & 3
10~21% of full-rated power	151 MW~318 MW	1
21~35% of full-rated power	319 MW~530 MW	2
35~48% of full-rated power	531 MW~727 MW	3
48~100% of full-rated power	738 MW~1515 MW	4

The number of AC filter injections at each bus 2 and bus 3 is 1 when LCC-HVDC system operates at 151 MW to 318 MW corresponding to 10% to 21% of full-rated power. In other words, the number of AC filter injection increases proportionally to the LCC-HVDC

operating point. This feature of LCC-HVDC system related with the AC filter injection is an important factor in analyzing TOV to determine the MOV surge arrester.

AC transmission double lines are installed between bus 1 and 2 as depicted in Figure 1. When the double-line fault (N-2 contingency) occurs, it could cause sub-synchronous torsional interaction (SSTI) between generators and LCC-HVDC systems in series or overloading on the LCC-HVDC transmission line that is the only inter-supply path in order to provide the active power produced from the three generators. To mitigate such a fault propagation as well as more severe fault impacts, it should be necessary to establish a remedial approach that includes the three generators trip and the LCC-HVDC system blocking action through special protection system (SPS). The SPS strategy is to trip the generators and block the LCC-HVDC system after tripping the double line. As seen in Figure 2, the fault condition maintains for T_0 and then circuit breakers (CBs) on the AC double line operates for an instant, which is a grid code for securing the power system reliability and resiliency. After the $T_1 - T_0 + T_2$ postponed from the CBs open, the signal of SPS reaches the generators and LCC-HVDC system, respectively. The postponed time implies a physical communication transfer time as an unintentional delay. It is also required for T_3 to tripping the AC filter from the grid, because the mechanical operation of the trip behavior should be unavoidable with its trip signal transfer.

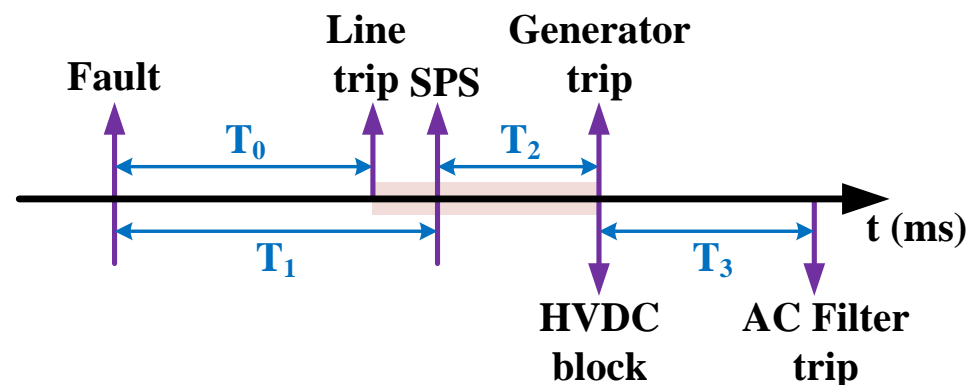


Figure 2. Double-line fault scenario between bus 1 and bus 2 shown in Figure 1 for analysis of temporary transient overvoltage (TOV) with respect to MOV surge arrester with LCC-HVDC transmission system with special protection system.

As a result, during the double-line fault contingency between bus 1 and bus 2, the remaining voltage sources cause a temporary transient overvoltage (TOV), and thus the TOV would not disappear, even though electrical path and voltage sources are disconnected from the grid. Although all supply paths are tripped, the AC filter still remained to the grid, and hence the inevitable situation results in an unpredictable aggravation on the overvoltage peak, duration, and pattern. To mitigate the TOV issue, the surge arrester could be placed at the buses adjacent to the critical equipment as illustrated in Figure 1. Therefore, an accurate rating design of the MOV surge arrester for absorbing the injected fault energy should be needed according to many comprehensive fault scenarios with grid conditions and the LCC-HVDC system. Furthermore, a detailed analysis method and procedure for determining an accurate rating of the MOV surge arrester in LCC-HVDC system should be required.

3. Metal-Oxide Varistor (MOV) Surge Arrester

A selection method of MOV surge arrester has been well introduced in the manufacturer's guide manual, and there have been general design methods in previous white papers [57–59]. A specific design and selection method for the surge arrester installed in LCC-HVDC system should be required due to a new philosophy in electrical power transmission integrated with power electronic-interfaced devices. This research is to focus on the changing characteristics such as amplitude, pattern, and duration of TOV highly

relying on LCC-HVDC operation with regard to the grid condition. The number of the MOV devices, which are capable of enduring the thermal explosion, should be determined through a comprehensive analysis based on generators' operating capacity, trip time of the passive filters, communication time delay owing to the SPS, and LCC-HVDC operating point. For analyzing the TOV caused by a severe fault such as N-2 contingency, a high-fidelity simulation should be conducted to distinguish a lightening, switching impulse and power frequency temporary overvoltage domain, respectively. According to the IEC-60071-1 international standard regarding definitions, principles, and rules of insulation coordination, the voltage classes could be classified according to shapes and frequency duration of transient voltage [60]. Based on the international standard, the categorization between impulses and temporary voltage domain could be distinguished by a range of voltage or overvoltage shape. Therefore, an elaborate analysis of transient overvoltage should be required for protecting the LCC-HVDC system with a surge arrester without the thermal energy explosion phenomenon from the transient overvoltage, and then the number of metal-oxide resistor stack would be determined. The rated voltage to withstand a thermal explosion is indicated in Table 3 based on a high-voltage test over metal-oxide resistor exploited in this research. In addition, the results of testing the withstand voltage of MOV corresponding to time and overvoltage is described in Table 4.

Table 3. Specification of metal-oxide varistor surge arrester.

Items	Value
Rated voltage	288 kV
Nominal discharge current	10 kA
Maximum continuous operating voltage	230 kV
Power frequency	60 Hz
Long-term insulation class	class 3
Power-frequency withstand voltage (Insulation Level)	450 kVrms
lightening withstand voltage (Insulation Level)	1.175 kV
Switching impulse withstand voltage (Insulation Level)	950 kVp
Metal-oxide resistor stack voltage	5.15 kV

Table 4. Test result of withstand voltage of MOV resistor stack.

Items	Value		
Maximum rated voltage (line-to-line)	362 kV		
Maximum rated voltage (RMS)	209 kV		
Maximum rated voltage (Peak)	295.6 kV		
Rated voltage of metal-oxide resistor stack	5.15 kV(@100sec)	5.55 kV(@10sec)	5.86 kV(@1sec)
No. of stack	56		
Total voltage (RMS)	288.4 kV	310.8 kV	328.16 kV
Total voltage ratio (p.u.)	1.38	1.49	1.57

4. Procedure of Metal Oxide Varistor (MOV) Surge Arrester Selection for LCC-HVDC System

In [61], a guideline regarding MOV surge arrester determination for HVDC converter stations was well defined. Based on the guideline, this paper proposes TOV study procedure for MOV surge arrester in LCC-HVDC transmission system and future power system with an increasing penetration level of RES. The TOV study is based on various influential factors affecting the large power system with an LCC-HVDC system. Figure 3 shows the proposed procedure of MOV surge arrester selection method for the LCC-HVDC system. The details of each stage would be explained in next sub-sections.

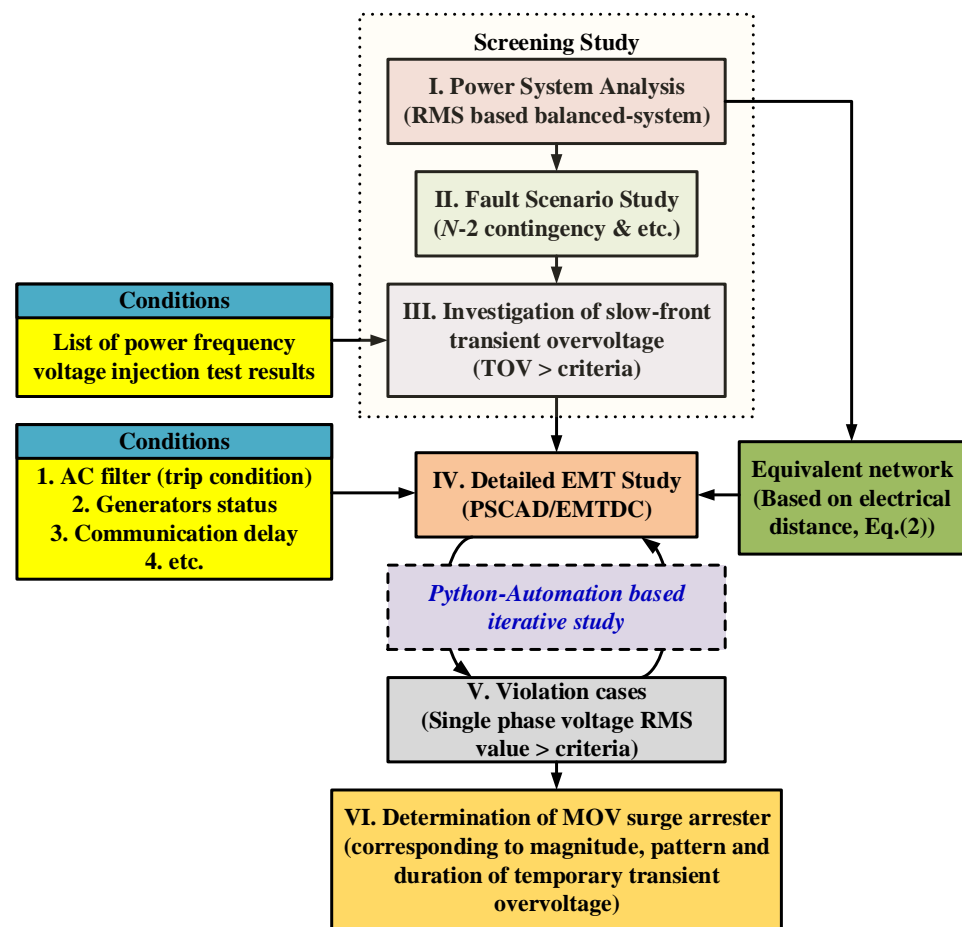


Figure 3. Procedure of MOV surge arrester selection for LCC-HVDC transmission system.

4.1. Power System Analysis

RMS-based power system analysis should be conducted according to an already planned power system operation strategy. As previously described in Section 2, the LCC-HVDC system operation condition could be considered from light load to peak load in accordance with generator operation conditions. Because the scenarios of LCC-HVDC system operation are determined by external factors (e.g., generators conditions, power system topologies, loadabilities, etc.) and then examined with many fault locations, a Python script-based application programming interface (API) shown in Figure 4 should be developed for automatically collecting and organizing a lot of data gathered from simulation results. This step is a necessary study phase for inspecting power system conditions as well as a fundamental process for selecting the MOV surge arrester. In other words, an automatic power system fault analysis platform should be prepared for obtaining the many required results one may need. The iterative study procedure shown in Figure 4 may be changed based on the purpose of developing the automatic platform.

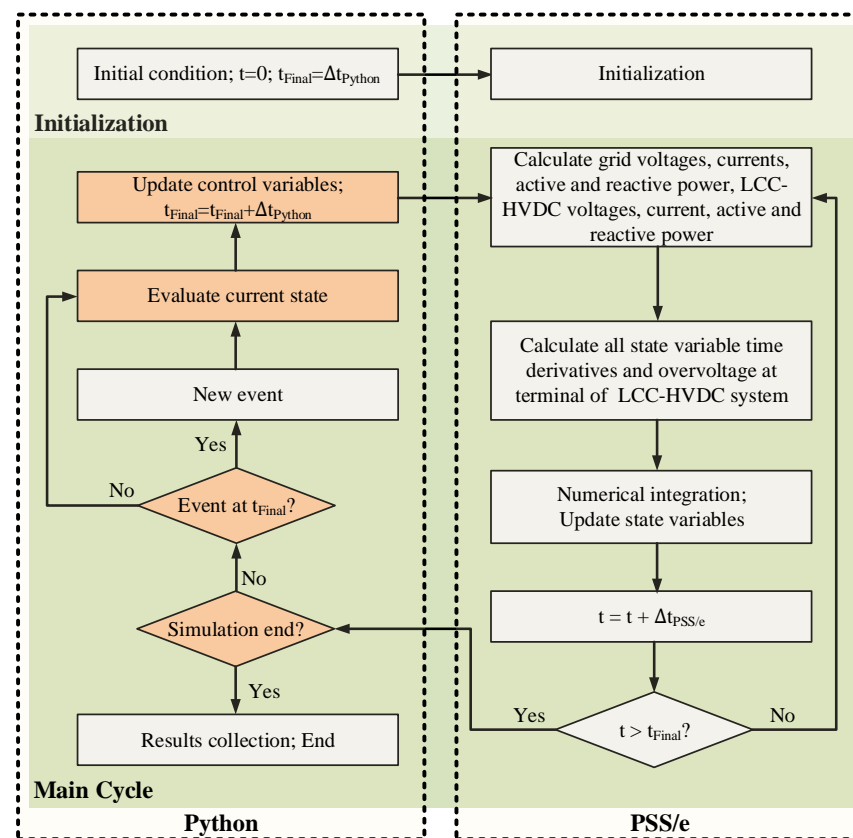


Figure 4. Iterative study method through Python-based API with PSS/e [62]. “Rights: openAccess”.

4.2. Fault Scenario Study

Among those many cases represented in power system analysis of previous step, N-2 contingency between bus 1 and bus 2 is selected in this paper highly related with TOV for MOV surge arrester. The right side of the grid at bus 3 is not considered because the installed STATCOM is able to support the system voltage regulation and hence TOV is less affected by faults near LCC-HVDC system. Furthermore, the main generator sources are not located near bus 3; as a result, the cases are excluded for comprehensively analyzing both generator operation and LCC-HVDC system with SPS. Thus, the left side of LCC-HVDC system is focused to discover main factors to have an impact on TOV. In summary, critical fault scenarios should be chosen in this stage based on a criterion that is accounted for requirements of grid reliability depending on each individual country, and then specific cases for TOV are designated with influential factors of the grid voltage.

4.3. Investigation of Slow-Front Transient Overvoltage

A screening study by transient and stability analysis (TSA) is conducted with respect to the N-2 contingency chosen by a previous step with reliability criterion. As indicated in Table 4, an initial condition of 1.57 p.u. withstands voltage with 57 metal-oxide resistor stacks of the surge arrester by an experimental test for power-frequency temporary TOV applied in this stage. More specific cases could be sorted with the 1.57 p.u. criterion. Moreover, slow-front transient overvoltage (SFTOV) is especially considered in the RMS-based analysis stage, because temporary TOV has been validated by an experimental test of thermal explosion at 100 ms, and the SFTOV is continuously maintained from 1 to 100 ms in Figure 5 and IEC-60071-1 also provides a classification of SFTOV to temporary transient overvoltage categorization. Therefore, for the screening study, an absolute value of SFTOV is employed as an index for sorting specific cases that need to be further investigated in detail with rigorous EMT simulation.

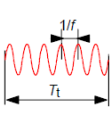
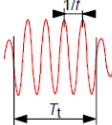
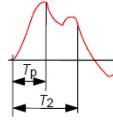
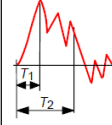
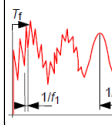
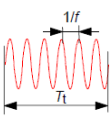
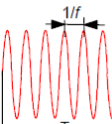
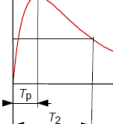
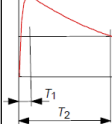
Class	Low frequency		Transient		
	Continuous	Temporary	Slow-front	Fast-front	Very-fast-front
Voltage or over-voltage shape					
Range of voltage or over-voltage shape	$f = 50\text{Hz}$ or 60Hz $T_t \geq 3600\text{s}$	$10\text{Hz} < f < 500\text{Hz}$ $0.02\text{s} \leq T_t \leq 3600\text{s}$	$20\mu\text{s} < T_p \leq 5000\mu\text{s}$ $T_2 \leq 20\text{ms}$	$0.1\mu\text{s} < T_1 \leq 20\mu\text{s}$ $T_2 \leq 300\mu\text{s}$	$T_t \leq 100\text{ns}$ $0.3\text{MHz} < f_1 < 100\text{MHz}$ $30\text{kHz} < f_2 < 300\text{kHz}$
Standard voltage shape	 $f = 50\text{Hz}$ or 60Hz	 $48\text{Hz} \leq f < 62\text{Hz}$ $T_t = 60\text{s}$	 $T_p = 250\mu\text{s}$ $T_2 = 2500\mu\text{s}$	 $T_1 = 1.2\mu\text{s}$ $T_2 = 50\mu\text{s}$	
Standard withstand voltage test		Short-duration power frequency test	Switching impulse test	Lighting impulse test	

Figure 5. Classes and shapes of overvoltages, standard voltage shapes, and standard withstand voltage tests [60]. “Copyright © 2019 IEC Geneva, Switzerland (www.iec.ch)”.

4.4. Equivalent Network

A detailed power system model should be developed through the equivalent network translation method for more specific LCC-HVDC system control in a large power system [63]. For a detailed EMT simulation model development, the large power system should be divided to simulate the complicated LCC-HVDC system [64–66]. That is, the power system model reduction should be conducted, and hence electrical distance is applied in this stage. An index for the electrical distance could be calculated by [67]

$$D_{ij} = -\log_{10} \left(\frac{\Delta U_i}{\Delta U_j} \right) \quad (1)$$

$$\left(\frac{\Delta U_i}{\Delta U_j} \right) = \frac{\left(\frac{\partial U}{\partial Q} \right)_{ij}}{\left(\frac{\partial U}{\partial Q} \right)_{jj}}, \quad (2)$$

where D_{ij} is an index for electrical distance between i -bus and j -bus, $U_{i,j}$ is each i, j bus voltages, and $Q_{i,j}$ is a reactive power. The electrical distance indicates a relationship between a certain bus voltage variation and other buses in accordance with the reactive power variation. By using the index, boundary buses are finally determined to include the large simulation model in the EMT platform. In general, a power system model reduction is performed with study requirements through a specific purpose [63–67]. However, in this research, the boundary buses are chosen only by electrical distance due to the purpose of transient overvoltage impact analysis during faults. In addition, the equivalent network is translated through E-Tran software by Electranix [68].

4.5. Detailed Electro-Magnetic Transient (EMT) Study

The equivalent network by large power system reduction method is developed with models of detailed synchronous generators, LCC-HVDC system, AC passive filters, and a more detailed control algorithm and sequences, as shown in Figure 1. The LCC-HVDC system model includes a specific controller from a certain manufacturer, and fault scenarios based on Figure 2 are applied with generators and LCC-HVDC system operation conditions. The operating capacity of the LCC-HVDC system depends on the number of generator operations, and the AC filters operate according to the required HVDC operating point. Requirements of fault conditions are reflected by generators, AC filters, and communication delay from the SPS in steady state of the LCC-HVDC system. In a detailed EMT analysis, TOV should be observed and analyzed under the designated conditions, which implies that the EMT study also has a difficult task for applying a lot of conditions in the simulation platform. Therefore, an API should be developed, such as in TSA-based power system analysis, which is possible by a Python automation iterative study based on API provided from the PSCAD/EMTDC simulation platform shown in Figure 6. As a result, automatic simulation platform development is required to repeatedly perform the simulations corresponding to parameters and grid operating conditions. The developed simulation platform could provide magnitude, pattern, and duration of TOV to be examined in detail.

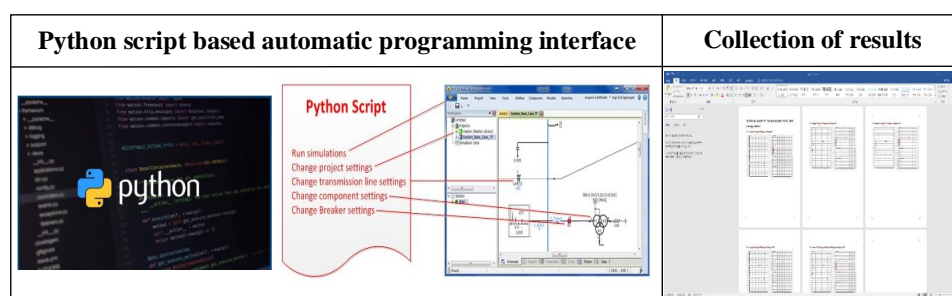


Figure 6. Python script-based detailed PSCAD/EMTDC iterative study method [69].

4.6. Classification of Violation Cases

As previously mentioned in Section 2, violated cases for 1.57 p.u. criterion on power-frequency overvoltage of TOV according to IEC-60071-1 are sorted. In a screening study, the violated cases are sorted based on a three-phase, RMS-based absolute value owing to balanced system. On the other hand, in a detailed EMT study, the distinct, single-phase RMS absolute value should be measured because the surge arrester is installed per each individual phase in general. Therefore, the detailed EMT study distinguishes violated cases with TOV over 1.57 p.u for 1 to 100 ms.

4.7. Determination of Metal-Oxide Resistor Stack

The 1.57 p.u. criterion could classify the violated cases with respect to the guaranteed withstand voltage from 57 metal-oxide resistor stacks in Table 4. The several cases among the violated cases are not included in a consideration of stacks' determination if they are not in LCC-HVDC operation strategy; however, a higher rated voltage surge arrester should be installed through more metal-oxide resistor stacks for over 1.57 p.u. criterion if they are unavoidable due to the necessary operation scenario. Finally, the resulted TOV pattern, magnitude, and duration could provide a detailed thermal energy absorbing capacity, and thus a more sufficient MOV surge arrester could be determined through the calculation such as in [49,59] with the TOV. The procedure of surge arrester selection for metal-oxide resistor stacks would be verified in Section 4.

5. Simulation Results

Based on the procedure of MOV surge arrester selection for LCC-HVDC system shown in Figure 3, the scenario-based cases are investigated in the specific power system

configuration illustrated in Figure 1. The first step is conducted for determining violated cases applied with the TOV criterion through a screening study by three-phase RMS-based simulation platform explained in Figure 4. As a result, three representative cases are determined for validating the proposed selection procedure of MOV; (Case I) above 1.57 p.u. criterion, (Case II) approximately 1.57 p.u. criterion, and (Case III) below 1.57 p.u. criterion of the SFTOV. The simulation results are shown in this Section 4.

5.1. Screening Study Results

As mentioned in previous Sections 4.1 and 4.2, the fault scenario study is conducted by a TSA tool to obtain the specific cases violating the 1.57 p.u. criterion of metal oxide resistor stack introduced in Section 2. Figure 7 shows the three cases to verify the selection procedure of MOV surge arrester; Case I exceeds the 1.57 p.u. criterion much more. Case II is a slight violation and should be investigated through detailed EMT study to ensure the pattern, magnitude, and duration of TOV. Case III is a non-violation below the 1.57 p.u. criterion and not considered for more detailed EMT study.

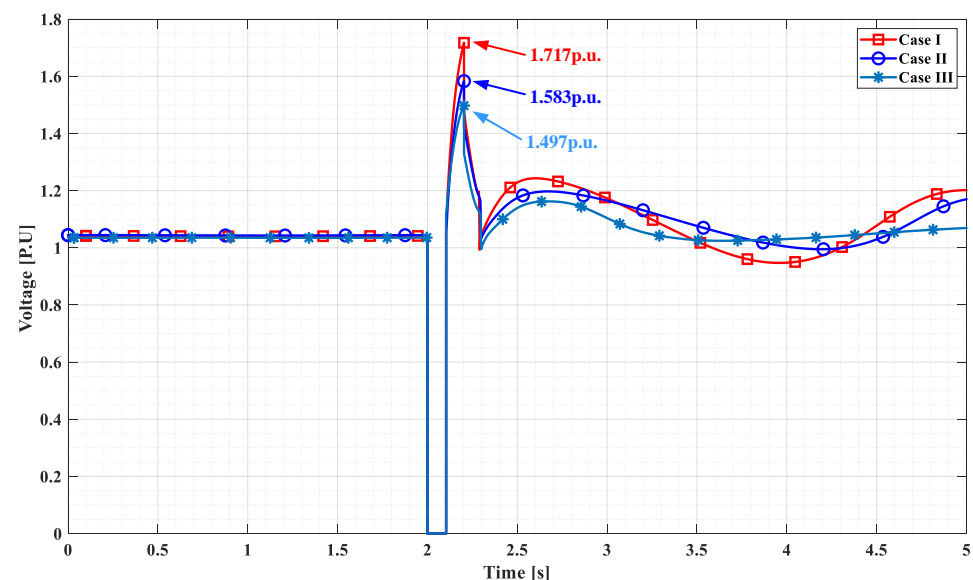


Figure 7. RMS-based TSA simulation results for screening study to obtain violated cases.

The simulation results could provide an SFTOV to screen the cases violating 1.57 p.u. criterion. From the power system analysis results, more detailed EMT simulation is conducted based on various conditions: (1) EMT simulation time step; (2) SPS signal transfer time delay; (3) AC filter mechanical switch open time delay; (4) interface transfer tap changer status; and (5) generator operation & LCC-HVDC system operation conditions.

5.2. Detailed Electro-Magnetic Transient (EMT) Study Results

A reduced equivalent power system is applied in detailed TOV analysis through PSCAD/EMTDC simulation. Figure 8 shows the PSCAD/EMTDC model for detailed TOV study with LCC-HVDC control and operation sequences. Figure 8a is an equivalent circuit for a complex transmission system. Figure 8b is a detailed generator model including practical generator dynamic files used in TSA tool, and Figure 8c is a 12-pulsed thyristor-based rectifier model for LCC-HVDC system.

Based on the reduced simulation model shown in Figure 8, detailed EMT studies are conducted with fault sequence shown in Figure 2, and the purpose of EMT simulation study is to analyze the influential factors affecting the TOV's pattern, magnitude, and duration. Hence, Case III is adopted in order to include additional violated cases through the discovery of more detailed TOV shapes and to verify the screening study with the SFTOV indicator. Case I and II should be definitely investigated to select a more accurate

number of resistor stacks. However, only Case III results would be shown due to the purpose of verifying the MOV selection method focused on in this paper.

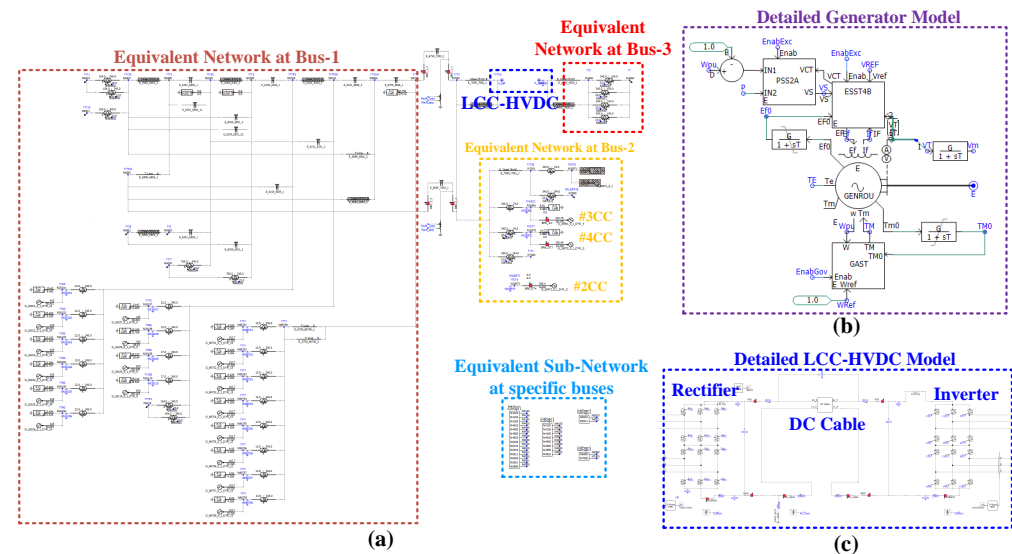


Figure 8. The PSCAD/EMTDC model for detailed TOV study by LCC-HVDC control and fault sequence. (a) Equivalent circuit. (b) Detailed generator model. (c) Thyristor-based 12-pulsed symmetric monopole LCC-HVDC system model.

5.2.1. Electro-Magnetic Transient (EMT) Simulation Time Step

Both conditions of 100 μ s and 10 μ s for simulation time step are compared, and the result is as shown in Figure 9. The result implies that the simulation time step for detailed EMT study does not affect the TOV during N-2 contingency. Therefore, an appropriate simulation time step only needs to be applied for ensuring the reliable simulation performance and the simulation time step, 50 μ s, is adopted in this paper.

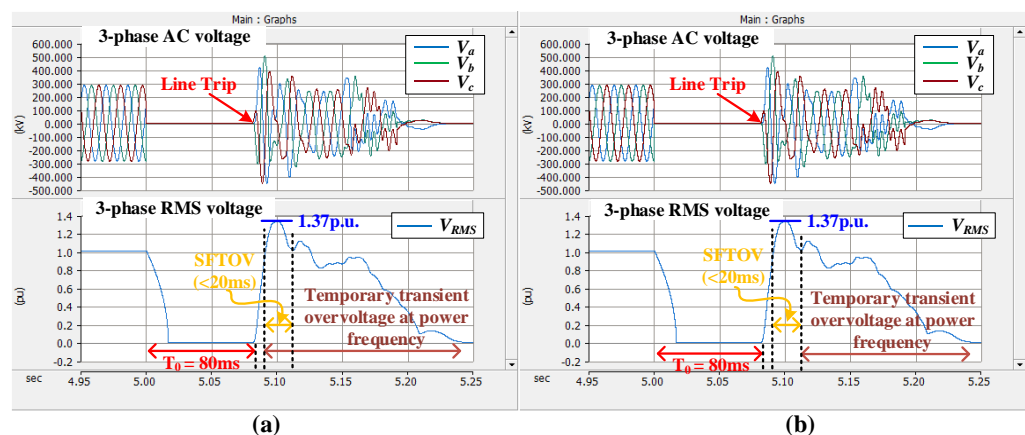


Figure 9. PSCAD/EMTDC simulation results according to EMT simulation time step. (a) 100 μ s and (b) 10 μ s.

5.2.2. Special Protection System (SPS) Signal Transfer Delay

The double-line fault contingency maintains for $T_0 = 80$ ms and the communication signal of SPS is delayed for $T_1 - T_0 + T_2$ to trip the generator and LCC-HVDC system. The communication delay causes TOV's pattern variation; however, this does not affect the SFTOV's first peak value shown in Figure 10. As seen in Figure 10, the SFTOV 1.57 p.u. criterion for distinguishing the violated cases is not affected, which implies that the condition may have an effect on the number of MOV resistor stacks for absorbing fault explosion energy.

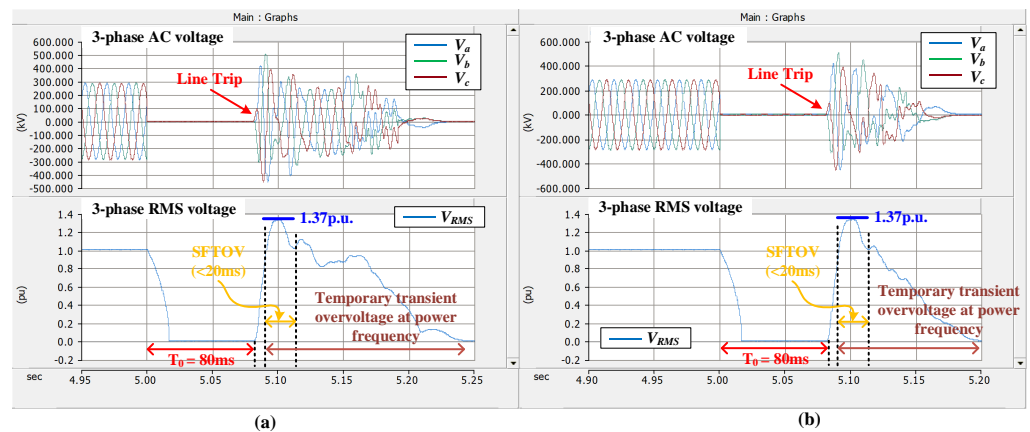


Figure 10. PSCAD/EMTDC simulation results according to SPS signal transfer time delay. (a) 70 ms and (b) 20 ms.

5.2.3. AC Filter Open Time

As shown in Figure 11, the mechanical switching open time delay for tripping the AC filters could result in the additional transient overvoltage variation. The reason is that the capacitive power of the AC passive filters could not have been consumed by inductive power injection due to the LCC-HVDC system that is already tripped. Therefore, the almost identical TOV second peak is generated, which means that the additional TOV second peak value has an impact on determination of the MOV surge arrester resistor stacks. As a result, the inevitable mechanical switch open time of AC filter should be considered at the stage of detailed EMT study and an experimentally measured switching open time also should be previously ensured for TOV study.

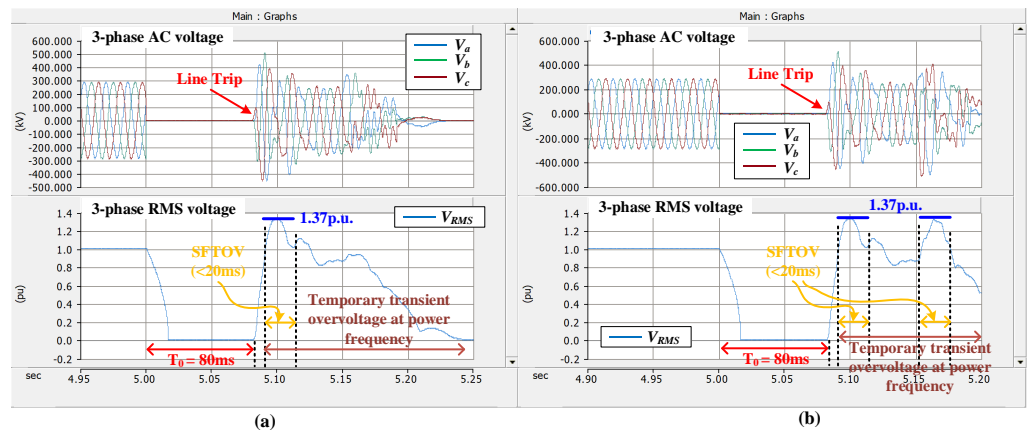


Figure 11. PSCAD/EMTDC simulation results according to AC filter mechanical switch open time delay. (a) No time delay and (b) 60 ms.

5.2.4. Interface Transformer Tap Changer Status

As shown in Figure 12, the interface transformer tap changer status has caused an approximate 4% peak value and duration increments of TOV. It implies that the AC voltage state highly depends on the power system condition having an effect on a proportional magnitude variation of TOV, not its pattern. Thus, a maximum tap changer status should be considered as a worst case to prevent it from thermal energy explosion.

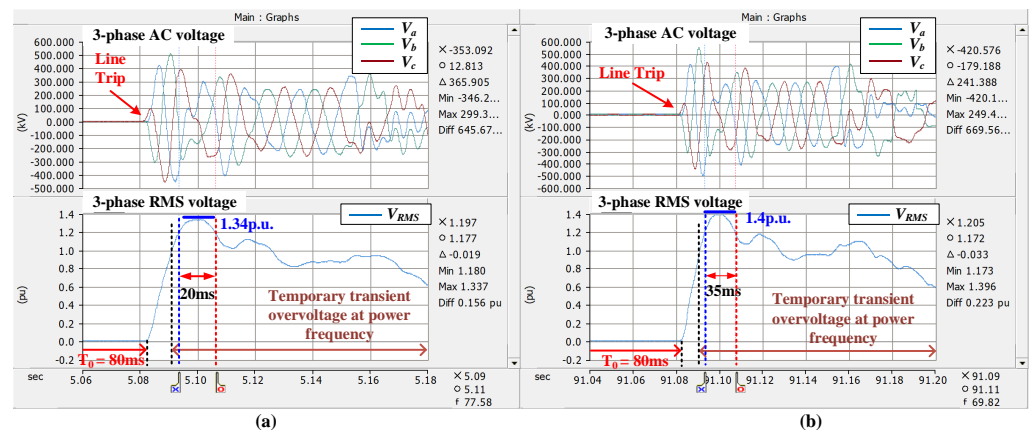


Figure 12. PSCAD/EMTDC simulation results according to interface transfer tap changer status. (a) Before interface transformer tap change and (b) after tap changer 1% increase.

5.2.5. Generator Operation and LCC-HVDC System Operation Conditions

The LCC-HVDC system operation capacity depends on the three generator operation conditions depicted in Figure 1. Moreover, the number of AC filter injection highly relies on the LCC-HVDC system operating point shown in Table 2. The discrete-featured operation of the AC passive filters results in an imbalanced inductive and capacitive power difference, which means that a certain operating point of the LCC-HVDC system moves a more compensating capacitive mode into the power system network. As a result, as shown in Figure 13, the TOV magnitude peak value in a 740-MW operation (four AC filters injection at 48% of full-rated power of LCC-HVDC system) is larger than in a 730-MW operation, which is in the operation state of three AC filters described in Table 2. That is, it implies that the TOV magnitude peak value highly depends on generators and LCC-HVDC system operation conditions, which should be definitely considered in the scenario-based TOV study.

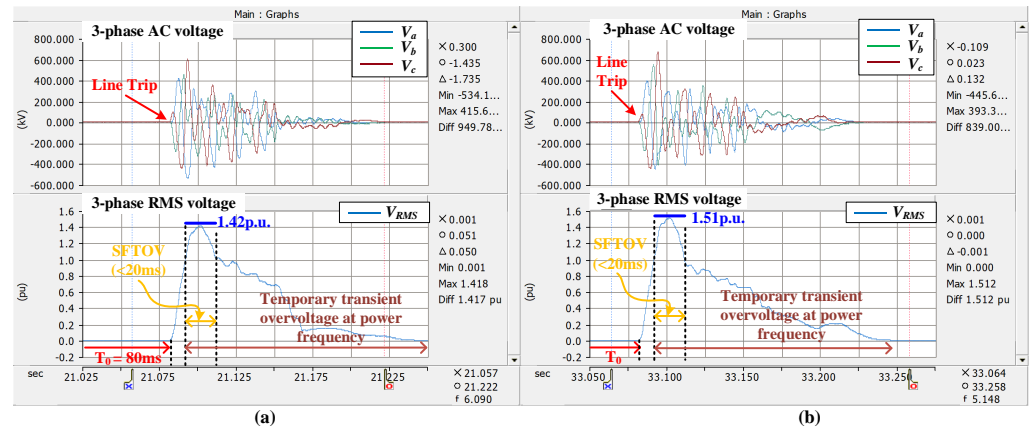


Figure 13. PSCAD/EMTDC simulation results according to generator operation and LCC-HVDC system operation conditions. (a) The 730-MW operating condition of LCC-HVDC system and (b) the 740-MW operation at 48% of full-rated power of LCC-HVDC system.

5.3. Discussion

To determine the MOV surge arrester resistor stacks for TOV in the LCC-HVDC transmission system, several influential factors should be considered in the detailed EMT study as follows:

- EMT simulation time step does not affect a significant TOV variation;
- SPS signal transfer time delay affects TOV's pattern and duration variation;
- AC filter mechanical switch open time delay affects TOV's pattern and duration variation and is a significant impact factor;

- Interface transformer tap changer status affects TOV's peak value and duration variation and the correlation is proportional; and
- generator operation and LCC-HVDC system operation conditions affects TOV's peak value variation and is a significant impact factor.

Based on the detailed EMT study, more accurate TOV phenomena could be analyzed after the screening study by power system analysis. In addition, the simulation results show that the RMS-based TOV could be compromisingly enough for filtering several violated cases to be more investigated. However, single-phase RMS value is much more important as mentioned in Section 4.2, because the MOV surge arrester is installed per each individual phase. As shown in Figure 14, the three-phase TOV RMS peak value does not exceed the 1.57 p.u. criterion; however, a specific single-phase RMS TOV could reach almost the TOV criterion and the all single-phase RMS voltage is different. Therefore, each individual RMS TOV magnitude should be an indicator to finally determine the maximum number of MOV surge arrester resister stacks for preventing it from an accumulated thermal energy explosion.

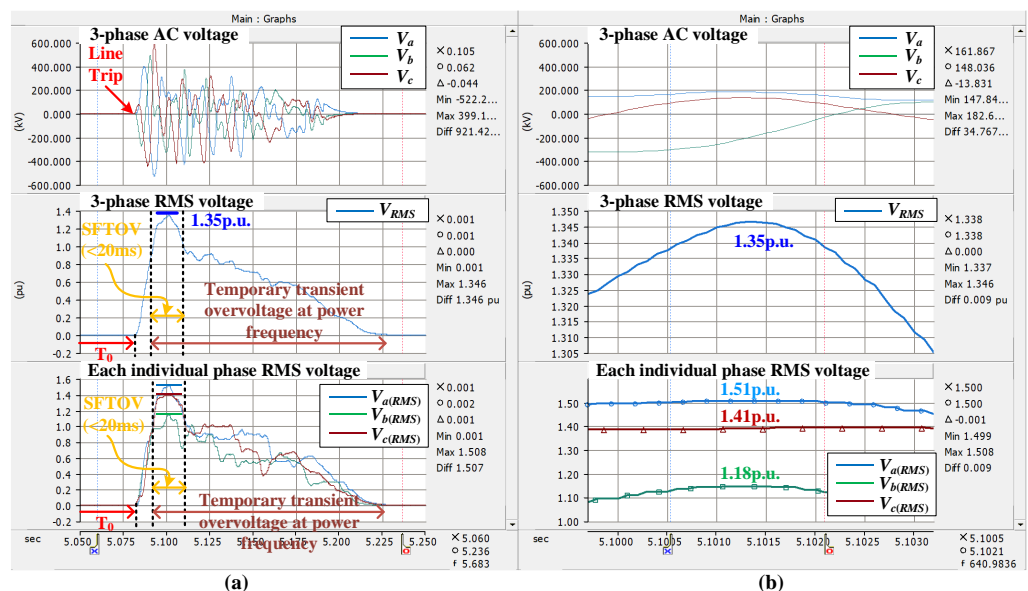


Figure 14. PSCAD/EMTDC simulation results for comparison of single phase RMS value. (a) Zoomed-out results and (b) zoomed-in results.

6. Conclusions

This paper has covered TOV phenomena analysis in a specific power system with LCC-HVDC transmission system and observed that the TOV phenomena highly depends on power system condition and LCC-HVDC system operation. In this paper, several influential factors were investigated by analyzing TOV for an MOV surge arrester, and thus a quite acceptable selection procedure of MOV surge arrester in LCC-HVDC system was proposed. The efficacy of the reasonable determination method was validated based on a practical situation and several scenarios, and hence the research results would help many utilities and TSO in developing LCC-HVDC transmission system engineering technology.

Funding: This research was supported by Korea Electrotechnology Research Institute (KERI) Primary research program through the National Research Council of Science & Technology (NST) funded by the Ministry of Science and ICT (MSIT) (No.22A01026).

Data Availability Statement: Not applicable.

Conflicts of Interest: The author declares no conflict of interest.

References

1. Xu, Z.; Voloh, I.; Khanbeigi, M. Evaluating The Impact of Increasing System Fault Currents on Protection. In Proceedings of the 70th Annual Conf. for Protective Relay Engineers (CPRE), College Station, TX, USA, 3–6 April 2017; pp. 1–20.
2. Alam, M.S.; Abido, M.A.Y.; El-Amin, I. Fault Current Limiters in Power Systems: A Comprehensive Review. *Energies* **2018**, *11*, 1025. [\[CrossRef\]](#)
3. Keller, J.; Kroposki, B. *Understanding Fault Characteristics of Inverter-Based Distributed Energy Resources*; Technical Report NREL/TP-550-46698; National Renewable Energy Lab. (NREL): Golden, CO, USA, 2007.
4. Adnan, A.Z.; Yusoff, M.E.; Hashim, H. Analysis on the Impact of Renewable Energy to Power System Fault Level. *Ind. J. Electr. Eng. Comput. Sci.* **2018**, *11*, 652–657. [\[CrossRef\]](#)
5. Liu, X. Fault Current Negative Contribution Method for Inverter-Based Distributed Generators Under Grid Unbalanced Fault. *IEEE Access* **2020**, *8*, 220807–220815. [\[CrossRef\]](#)
6. Boljevic, S.; Conlon, M.F. The Contribution to Distribution Network Short-Circuit Current Level From The Connection of Distributed Generation. In Proceedings of the 43rd International Universities Power Engineering Conference, Padua, Italy, 1–4 September 2008; pp. 1–6.
7. Rahimi, S.; Wiechowski, W.; Randrup, M.; Ostergaard, J.; Nielsen, A.H. Identification of Problems when Using Long High Voltage AC Cable in Transmission System II: Resonance & Harmonic Resonance. In Proceedings of the 2008 IEEE/PES Transmission and Distribution Conference and Exposition, Chicago, IL, USA, 21–24 April 2008; pp. 1–8.
8. *Advanced Transmission Technologies*; Technical Report; United States Department of Energy: Washington, DC, USA, 2020, p. 20585.
9. Soland, M.; Loosli, S.; Koch, J.; Christ, O. Acceptance Among Residential Electricity Consumers Regarding Scenarios of A Transformed Energy System in Switzerland—A Focus Group Study. *Energy Effic.* **2018**, *11*, 1673–1688. [\[CrossRef\]](#)
10. Maarten, W. The Research Agenda on Social Acceptance of Distributed Generation in Smart Grids: Renewable as Common Pool Resources. *Renew. Sustain. Energy Rev.* **2012**, *16*, 822–835.
11. Maarten, W. Social Acceptance, Lost Objects, And Obsession with The “Public”—The Pressing Need for Enhanced Conceptual And Methodological Rigor. *Energy Res. Soc. Sci.* **2019**, *48*, 269–276.
12. Harrouz, A.; Belatrache, D.; Boulal, K.; Colak, I.; Kayisli, K. Social Acceptance of Renewable Energy dedicated to Electric Production. In Proceedings of the 9th International Conference on Renewable Energy Research and Application (ICRERA), Glasgow, UK, 27–30 September 2020; pp. 283–288.
13. Zaunbrecher, B.; Ziefle, M. Social Acceptance and Its Role for Planning Technology Infrastructure—A Position Paper, Taking Wind Power Plants as an Example. In Proceedings of the 4th International Conference on Smart Cities and Green ICT Systems, Lisbon, Portugal, 20–22 May 2015.
14. Liu, G.; Li, Y. Current Status and Key Issues of HVDC Transmission Research: A Brief Review. In Proceedings of the 7th International Symposium on Mechatronics and Industrial Informatics (ISMII), Zhuhai, China, 22–24 January 2021; pp. 16–19.
15. Tosatto, A.; Weckesser, T.; Chatzivasileiadis, S. Market Integration of HVDC Lines: Internalizing HVDC Losses in Market Clearing. *IEEE Trans. Power Syst.* **2020**, *35*, 451–461. [\[CrossRef\]](#)
16. Wang, S.; Tang, G.; He, Z. Comprehensive Evaluation of VSC-HVDC Transmission Based on Improved Analytic Hierarchy Process. In Proceedings of the Third International Conference on Electric Utility Deregulation and Restructuring and Power Technologies, Nanjing, China, 6–9 April 2008; pp. 2207–2211.
17. Ayo, A.M.; Ríos, M.A. Alternatives of Development of SINEA Project in VSC-HVDC. In Proceedings of the IEEE/PES Transmission and Distribution Conference and Exposition (T&D), Chicago, IL, USA, 12–15 October 2020; pp. 1–5.
18. *Assessing HVDC Transmission for Impacts of Non-Dispatchable Generation*; Technical Report; United States Department of Energy: Washington, DC, USA, 2018, p. 20585.
19. Alassi, A.; Bañales, S.; Ellabban, O.; Adam, G.; MacIver, C. HVDC Transmission: Technology Review, Market Trends and Future Outlook. *Renew. Sustain. Energy Rev.* **2019**, *112*, 530–554. [\[CrossRef\]](#)
20. Okba, M.H.; Saied, M.H.; Mostafa, M.Z.; Abdel-Moneim, T.M. High Voltage Direct Current Transmission—A Review, Part I. In Proceedings of the 2012 IEEE Energytech, Cleveland, OH, USA, 29–31 May 2012; pp. 1–7.
21. Sessa, D.; Sebastian, Antonio, C.; Roberto, B. Availability Analysis of HVDC-VSC Systems: A Review. *Energies* **2019**, *12*, 2703. [\[CrossRef\]](#)
22. Watson N.R. An Overview of HVDC Technology. *Energies* **2020**, *13*, 4342. [\[CrossRef\]](#)
23. Huq, K.S.S.; Huq, K.R. A Technical Review on High Voltage Direct Current (HVDC) Transmission. *Int. J. Electr. Eng.* **2018**, *11*, 77–85.
24. Bahrman, M.P. HVDC Transmission Overview. In Proceedings of the 2008 IEEE/PES Transmission and Distribution Conference and Exposition, Chicago, IL, USA, 21–24 April 2008; pp. 1–7.
25. Bahrman, M.P. Overview of HVDC Transmission. In Proceedings of the IEEE/PES Transmission and Distribution Conference and Exposition, Caracas, Venezuela, 15–18 August 2006; pp. 18–23.
26. Lluch, J.R. *Modelling, Control and Simulation of LCC-HVDC Systems for Stability Studies*; Universitat Politècnica de Catalunya: Barcelona, Spain, 2017.
27. Oni, O.E.; Davidson, I.E.; Mbangula, K.N.I. A Review of LCC-HVDC and VSC-HVDC Technologies and Applications. In Proceedings of the IEEE 16th International Conference on Environment and Electrical Engineering (EEEIC), Florence, Italy, 7–10 June 2016; pp. 1–7.

28. Sharifabadi, K.; Harnefors, L.; Nee, H.-P.; Norrga, S.; Teodorescu, R. *Design, Control and Application of Modular Multilevel Converters for HVDC Transmission Systems*; John Wiley & Sons Ltd.: Hoboken, NJ, USA, 2016.
29. ALSTOM (Firm). *HVDC: Connecting to the Future*; Technical Report; Alstom Grid: Paris, France, 2010.
30. Kim, C.K.; Sood, V.K.; Jang, G.-S.; Lim, S.-J.; Lee, S.-J. *HVDC Transmission: Power Conversion Applications in Power Systems*; Wiley-IEEE Press: Piscataway, NJ, USA, 2009.
31. Kim, H.; Kim, J.-K.; Song, J.; Lee, J.; Han, K.; Shin, J.; Kim, T.; Hur, K. Smart and Green Substation: Shaping the Electric Power Grid of Korea. *IEEE Power Energy Mag.* **2019**, *17*, 24–34. [\[CrossRef\]](#)
32. Han, S. Calculating the Interface Flow Limits for the Expanded Use of High-Voltage Direct Current in Power Systems. *Energies* **2020**, *13*, 2863. [\[CrossRef\]](#)
33. Choi, D.; Lee, S.H.; Son, G.T.; Park, J.W.; Baek, S.M. Planning of HVDC System Applied to Korea Electric Power Grid. *J. Electr. Eng. Technol.* **2018**, *13*, 105–113.
34. Global HVDC, FACTS Leading Company, KAPES, HVDC Project. Available online: http://kapes.co.kr/eng/business/e_business03.asp#none (accessed on 20 September 2022).
35. Buk Danjin–Godeok Link to be Completed by 2020. Available online: <https://www.modernpowersystems.com/features/featurebuk-danjingodeok-link-to-be-completed-by-2020-7621501> (accessed on 20 September 2022).
36. Energy and Environment News. Available online: <https://www.e2news.com/news/articleView.html?idxno=216872> (accessed on 20 September 2022).
37. GE and KAPES Awarded Contract to Complete Final Phase of HVDC Energy Highway. Available online: <https://www.energyprojectstechnology.com/ge-and-kapes-awarded-contract-to-complete-final-phase-of-hvdc-energy-highway> (accessed on 20 September 2022).
38. Zhang, M.; Yuan, X.; Hu, J. Mechanism Analysis of Subsynchronous Torsional Interaction With PMSG-Based WTs and LCC-HVDC. *IEEE J. Emerg. Sel. Top. Power Electr.* **2021**, *9*, 1708–1724. [\[CrossRef\]](#)
39. Wei, X.; Hu, J. Sub-Synchronous Torsional Interaction with LCC-HVDC in DC Current Control Timescale. In Proceedings of the 8th Renewable Power Generation Conference (RPG 2019), Shanghai, China, 24–25 October 2019; pp. 1–7.
40. Gao, B.; Zhang, R.; Li, R.; Yu, H.; Zhao, G. Subsynchronous Torsional Interaction of Wind Farms with FSIG Wind Turbines Connected to LCC-HVDC Lines. *Energies* **2017**, *10*, 1435. [\[CrossRef\]](#)
41. Piwko, R.J.; Larsen, E.V. HVDC System Control for Damping of Subsynchronous Oscillation. *IEEE Trans. Power App. Syst.* **1982**, *PAS-101*, 2203–2211. [\[CrossRef\]](#)
42. Zhou, C.; Xu, Z. Damping Analysis of Subsynchronous Oscillation Caused by HVDC. In Proceedings of the 2003 IEEE PES Transmission and Distribution Conference and Exposition (IEEE Cat. No.03CH37495), Dallas, TX, USA, 7–12 September 2003.
43. Damas, R.N.; Son, Y.; Yoon, M.; Kim, S.Y.; Choi, S. Subsynchronous Oscillation and Advanced Analysis: A Review. *IEEE Access* **2020**, *8*, 224020–224032. [\[CrossRef\]](#)
44. Lee, C.-H.; Yun, J.-S.; Kwak, J.-s.; Choi, J.-h. *Study on Protection System of ± 500 kV HVDC System*; The Korean Institute of Electrical Engineers: Seoul, Korea, 2019.
45. Buk-Dangjin – Godeok Transmitting Power to Cities GE’s HVDC Technology to Power a New Industrial City in South Korea. Available online: <https://www.gegridsolutions.com/products/applications/hvdc/hvdc-lcc-bukdangjin-casestudy-en-2019-07-grid-pea-0577.pdf> (accessed on 20 September 2022).
46. Ramadhan, U.F.; Suh, J.; Hwang, S.; Lee, J.; Yoon, M. A Comprehensive Study of HVDC Link with Reserve Operation Control in a Multi-Infeed Direct Current Power System. *Sustainability* **2022**, *14*, 6091. [\[CrossRef\]](#)
47. Yang, H.-S.; Kim, G.-D.; Yeo, G.-T.; Kim, K.-S. *The Engineering of Converter System for 500 kV HVDC Link Project Between Bukdangjin and Goduk*; The Korean Institute of Electrical Engineers: Seoul, Korea, 2016.
48. Yun, J.-H.; Hong, G.-Y.; Cho, H.-J.; Koo, B.-J. *The Production of Thyristor Valve for BukDangjin-Goduk HVDC*; The Korean Institute of Electrical Engineers: Seoul, Korea, 2017.
49. Milan, S. Selection of the Surge Arrester Energy Absorption Capability Relating to Lightning Overvoltages. In Proceedings of the 18th International Conference on Electricity Distribution, Turin, Italy, 6–9 June 2005; pp. 1–3.
50. Hinrichsen, V.; Reinhard, M.; Richter, B.; Göhler, R.; Greuter, F.; Holzer, M.; Ishibe, S.; Ishizaki, Y.; Johnnerfelt, B.; Kobayashi, M.; et al. Energy Handling Capability of High-Voltage Metal-Oxide Surge Arresters Part 1: A Critical Review of the Standards. In Proceedings of the Cigre International Technical Colloquium, Rio De Janeiro, Brazil, 12–13 September 2007.
51. Font, A.; İlhan, S.; Özdemir, A. Line Surge Arrester Application for A 380 kV Power Transmission Line. In Proceedings of the IEEE International Conference on High Voltage Engineering and Application (ICHVE), Chengdu, China, 19–22 September 2016; pp. 1–4.
52. Badrkhani Ajaei, F.; Iravani, R. Cable Surge Arrester Operation Due to Transient Overvoltages Under DC-Side Faults in the MMC–HVDC Link. *IEEE Trans. Power Deliv.* **2016**, *31*, 1213–1222. [\[CrossRef\]](#)
53. Gu, Y.; Huang, X.; Qiu, P.; Hua, W. Study of Overvoltage Protection and Insulation Coordination for MMC based HVDC. In Proceedings of the 2nd International Conference on Computer Science and Electronics Engineering (ICCSEE 2013), Hangzhou, China, 22–23 March 2013.
54. Xu, D.; Zhao, X.; Lu, Y.; Qin, K.; Guo, L. Study on Overvoltage of Hybrid LCC-VSC-HVDC Transmission. *J. Eng.* **2019**, *2019*, 1906–1910. [\[CrossRef\]](#)

55. Xu, J.; Zhu, S.; Li, C.; Zhao, C. The Enhanced DC Fault Current Calculation Method of MMC-HVDC Grid With FCLs. *IEEE J. Emerg. Sel. Top. Power Electr.* **2019**, *7*, 1758–1767. [CrossRef]
56. Yu, J.; Xu, Z.; Zhang, Z.; Song, Y. Hybrid HVDC Circuit Breakers with an Energy Absorption Branch of a Parallel Arrester Structure. *Instit. Eng. Technol.* **2021**, *7*, 197–207. [CrossRef]
57. Jonathan Woodworth. *Understanding Temporary Overvoltage Behavior of Arresters*, 2nd ed.; Technical Report of ArresterWorks; Jonathan Woodworth: Olean, NY, USA, 2017.
58. Surge Arrester Buyer's Guide Edition 4. Available online: [https://library.e.abb.com/public/837fb693e1d19a1dc1257b130057b22a/Buyers%20guide%20Selection%20\(C\).pdf](https://library.e.abb.com/public/837fb693e1d19a1dc1257b130057b22a/Buyers%20guide%20Selection%20(C).pdf) (accessed on 20 September 2022).
59. High Voltage Surge Arresters Buyer's Guide. Available online: <https://library.e.abb.com/public/ba61a5f190bf46fe8676554e0a2e9e4a/Buyer%27s%20Guide%20Surge%20Arresters%202019-10-17.pdf> (accessed on 20 September 2022).
60. IEC 60071-1; IEC International Standard. Insulation Co-Ordination—Part I: Definitions, Principles and Rules. iTeh, Inc.: Newark, DE, USA, 2019.
61. Ekstrom, A. *Guidelines for the Application of Metal Oxide Arresters without Gaps for HVDC Converter Stations*; Working Group 33/14.05; International Council on Large Electric Systems: Paris, France, 2005.
62. Pedro, M.; Pousada, D.; Pedro, A. Impact of Vehicle to Grid in the Power System Dynamic Behaviour. Ph.D. Thesis, Faculty of Engineering of University of Porto, Porto, Portugal, 2011.
63. Kim, S.; Kim, H.; Lee, H.; Lee, J.; Lee, B.; Jang, G.; Lan, X.; Kim, T.; Jeon, D.; Kim, Y.; et al. Expanding Power Systems in the Republic of Korea: Feasibility Studies and Future Challenges. *IEEE Power Energy Mag.* **2019**, *17*, 61–72. [CrossRef]
64. Lin, X.; Gole, A.M.; Yu, M. A Wide-Band Multi-Port System Equivalent for Real-Time Digital Power System Simulators. *IEEE Trans. Power Syst.* **2009**, *24*, 237–249. [CrossRef]
65. Zhang, Y.; Gole, A.M.; Wu, W.; Zhang, B.; Sun, H. Development and Analysis of Applicability of a Hybrid Transient Simulation Platform Combining TSA and EMT Elements. *IEEE Trans. Power Syst.* **2013**, *28*, 357–366. [CrossRef]
66. Liang, Y.; Lin, X.; Gole, A.M.; Yu, M. Improved Coherency-Based Wide-Band Equivalents for Real-Time Digital Simulators. *IEEE Trans. Power Syst.* **2011**, *26*, 1410–1417. [CrossRef]
67. Song, J.; Hur, K.; Lee, J.; Lee, H.; Lee, J.; Jung, S.; Shin, J.; Kim, H. Hardware-in-the-Loop Simulation Using Real-Time Hybrid-Simulator for Dynamic Performance Test of Power Electronics Equipment in Large Power System. *Energies* **2020**, *13*, 3955. [CrossRef]
68. E-Tran Software Electronix. Available online: <http://www.electronix.com/software/> (accessed on 20 September 2022).
69. PSCAD Automation Library. Available online: <https://www.pscad.com/software/pscad/automation-library> (accessed on 20 September 2022).